

# Journal of Biomedical Optics

BiomedicalOptics.SPIEDigitalLibrary.org

## **Low-level laser therapy on skeletal muscle inflammation: evaluation of irradiation parameters**

Matías Mantineo  
João P. Pinheiro  
António M. Morgado

**SPIE.**

# Low-level laser therapy on skeletal muscle inflammation: evaluation of irradiation parameters

Matías Mantineo,<sup>a,b</sup> João P. Pinheiro,<sup>c</sup> and António M. Morgado<sup>a,b,\*</sup>

<sup>a</sup>University of Coimbra, Instrumentation Center, Department of Physics, Coimbra 3004-516, Portugal

<sup>b</sup>BILI-Institute for Biomedical Imaging and Life Sciences, Azinhaga de Santa Comba-Celas, Coimbra 3000-548, Portugal

<sup>c</sup>University of Coimbra, Faculty of Medicine, Azinhaga de Santa Comba-Celas, Coimbra 3000-548, Portugal

**Abstract.** We evaluated the effect of different irradiation parameters in low-level laser therapy (LLLT) for treating inflammation induced in the gastrocnemius muscle of rats through cytokines concentration in systemic blood and analysis of muscle tissue. We used continuous (830 and 980 nm) and pulsed illuminations (830 nm). Animals were divided into five groups per wavelength (10, 20, 30, 40, and 50 mW), and a control group. LLLT was applied during 5 days with a constant irradiation time and area. TNF- $\alpha$ , IL-1 $\beta$ , IL-2, and IL-6 cytokines were quantified by ELISA. Inflammatory cells were counted using microscopy. Identical methodology was used with pulsed illumination. Average power (40 mW) and duty cycle were kept constant (80%) at five frequencies (5, 25, 50, 100, and 200 Hz). For continuous irradiation, treatment effects occurred for all doses, with a reduction of TNF- $\alpha$ , IL-1 $\beta$ , and IL-6 cytokines and inflammatory cells. Continuous irradiation at 830 nm was more effective, a result explained by the action spectrum of cytochrome c oxidase (CCO). Best results were obtained for 40 mW, with data suggesting a biphasic dose response. Pulsed wave irradiation was only effective for higher frequencies, a result that might be related to the rate constants of the CCO internal electron transfer process. © 2014 Society of Photo-Optical Instrumentation Engineers (SPIE) [DOI: 10.1117/1.JBO.19.9.098002]

Keywords: low-level laser therapy; inflammation; skeletal muscle; blood cytokines; irradiation parameters evaluation.

Paper 140205PR received Mar. 31, 2014; revised manuscript received Aug. 5, 2014; accepted for publication Aug. 19, 2014; published online Sep. 8, 2014.

## 1 Introduction

Low-level laser therapy (LLLT) is both an active research topic and an expanding clinical therapeutic technique. In addition to the need for more evidence on therapy results and adequate dose and beam parameters, it is still necessary to clarify the cellular mechanisms mediated by LLLT.<sup>1-4</sup> It is currently thought that the main mechanism of action results from photon absorption by mitochondrial chromophores, namely cytochrome c oxidase (CCO), leading to increased adenosine triphosphate (ATP) production and reduction of oxidative stress and restored mitochondrial function, starting a cascade of effects promoting tissue repair and reducing inflammation.<sup>5</sup>

There are several studies showing the therapeutic effect of LLLT on all stages of the skeletal muscle repair process after lesion.<sup>6-10</sup> In the acute inflammation phase, LLLT acts on mitochondria, increasing electron transfer along the electron transport chain and proton transport across the inner mitochondrial membrane. The consequence is a substantial rise in ATP production that leads to the reactivation of DNA, RNA and proteins synthesis, increasing cell proliferation.<sup>11-13</sup> During the inflammation phase, LLLT also plays an antioxidative role. The recruitment of immune cells, triggered by inflammatory mediators, is a necessary response for the phagocytosis of cellular debris. However, the higher number of neutrophils and macrophages in the injured area results in a greater concentration of reactive oxygen and nitrogen species (ROS and RNS).<sup>14</sup> As these oxidants modulate transcription factor NF- $\kappa$ B, which in turn regulates the expression of cytokines and chemokines that control the inflammatory

response,<sup>15</sup> a condition of oxidative unbalance can cause additional injury, amplifying the inflammatory response and expanding the injured area. LLLT promotes oxidative balance by increasing the levels of superoxide dismutase (SOD) enzyme. Higher expression of SOD causes less expression of cyclooxygenases and a lower release of prostaglandins. The interactions between SOD, RNS and ROS, subsequent to LLLT, seem to balance the oxidants' beneficial and harmful effects by reducing the oxidants concentration without compromising cell proliferation.<sup>9,16</sup>

There is evidence that LLLT also acts on the muscle repair phase, stimulating the activation of myogenic satellite cells and promoting angiogenesis.<sup>17-19</sup> The activation of satellite cells is regulated by growth factors such as transforming growth factor (TGF)- $\beta$ , basic fibroblast growth factor (FGFb), and insulin-like growth factor (IGF-1).<sup>20</sup> TGF- $\beta$  influences successful muscle repair since excessive production of this growth factor leads to a higher production of type I collagen and the formation of non-functional fibrotic tissue.<sup>20,21</sup> Activated satellite cells express more myogenic regulatory factors (MRFs). These MRFs induce differentiation of myoblasts into myocytes to regenerate skeletal muscle tissue.<sup>7,20-22</sup> Angiogenesis, which is fundamental for successful muscle regeneration, is regulated by vascular endothelial growth factor (VEGF). It was already shown that LLLT increases the expression of MRFs and VEGF expression while concurrently reducing TGF- $\beta$  and, consequently, collagen deposition and muscle fibrosis.<sup>23,24</sup>

LLLT effects in irradiated biological tissues depend directly on irradiation and treatment parameters such as wavelength, radiant power, irradiated area, and exposure time. From these parameters, it is possible to calculate radiant exposure or energy

\*Address all correspondence to: António Miguel Morgado, E-mail: miguelmorgado@uc.pt

dose (energy per irradiated area), irradiance, and total radiant energy. The published studies concerning LLLT for muscle repair present a considerable variety of irradiation and treatment parameters and protocols. Laser wavelengths vary between 632.8 and 904 nm. Therapeutic effects are reported<sup>25,26</sup> for radiant exposures from 1 J/cm<sup>2</sup> to more than 300 J/cm<sup>2</sup>. Protocols show a large variation in the number of treatment days and of daily treatment sessions.

Another important feature concerns the modality of radiation delivery: continuous wave (CW) or pulsed wave (PW). The most used modality is CW irradiation, which has been used for the whole range of LLLT applications. There is some evidence that PW irradiation can be more effective than CW illumination with equivalent irradiation and dosimetry parameters, particularly for wound healing and poststroke management applications.<sup>27</sup> As far as we know, no study was published concerning PW irradiation for skeletal muscle repair.

Here, we report on the effect of different LLLT doses, using both CW (830 and 980 nm) and PW irradiations (830 nm), in the inflammation phase of skeletal muscle injury, induced by mechanical trauma in the gastrocnemius muscle of Wistar rats. LLLT treatment effect was evaluated measuring the concentration of cytokines (TNF- $\alpha$ , IL-1 $\beta$ , IL-2, and IL-6) in systemic blood and through histological analysis of muscle tissue. Our goal was to evaluate treatment effectiveness with different irradiation parameters. First, we evaluated different energy doses for two distinct wavelengths with CW irradiation. Then, we compared CW and PW irradiations using the wavelength and average power that produced the largest treatment effect on the first experiment. Although our experiments were not designed to validate any of the LLLT action mechanisms, we discuss our results in the framework of the currently most accepted LLLT mechanism, based on the role of CCO as a primary photoacceptor for red-NIR radiation. Parts of this work were previously presented at SPIE BiOS 2014.<sup>28</sup>

## 2 Materials and Methods

### 2.1 Animals

We used 85 *Rattus norvegicus* (Wistar strain) male adult rats, with an average body mass of  $256.35 \pm 21.22$  g and 8 weeks of age. The rats were housed in collective standard cages (three animals per cage), with a controlled room temperature of 21°C, cage ventilation rates of about 75 air changes per hour and relative humidity of 70%. Bedding was replaced once a week.<sup>29,30</sup> All procedures were approved by the Commission of Ethics of the Faculty of Medicine of the University of Coimbra, which follows the Directive 2010/63/EU of the European Parliament and of the European Council.<sup>31</sup>

### 2.2 Trauma Induction

A controlled and reproducible inflammation condition between different animals was created, using the model of muscle trauma proposed by Rizzi et al.<sup>32</sup> Gastrocnemius muscle injury was induced by single impact, with a press developed by Industrias Mantineo, Mendoza, Argentina (Fig. 1), after shaving the animal's leg. Injury was done by a metal mass (0.300 kg) falling through a guide from a 30-cm height. The impact energy was 0.889 J. During the procedure, rats were anesthetized with a mixture of isoflurane (2.5%) and oxygen (97.5%) at a flow of 1.5 l/min. Inflammation was produced at day 0, starting



Fig. 1 Drop-mass press device for inflammation induction.

at 9:00 a.m. The average duration of the process was approximately 3 min per rat.

### 2.3 Laser Therapy

Laser radiation was administered using a Thorlabs ITC4001 Laser Diode/TEC Controller, with a single HL8338 GaAlAs laser diode (830 nm) or L9805E2P5 GaAlAs laser diode (980 nm) (Thorlabs, Newton, New Jersey, USA). Laser diode temperature was controlled.

The 830-nm wavelength was selected since it is a wavelength located in the band of highest transmission through the combination of skin and muscle (770–850 nm),<sup>33</sup> and is one of the two most common wavelengths used in therapeutic light sources (the other is 632.8 nm) and also is a peak of the CCO absorption spectrum, attributed to the relatively oxidized Cu<sub>A</sub> chromophores of CCO.<sup>34</sup> It is important to remember that the absorption spectrum of CCO is similar to the action spectra for biological responses to light, such as DNA and RNA synthesis, a fact that supports the role of CCO as a primary photoacceptor for red-NIR radiation in LLLT.

One of the reasons for selecting the 980-nm wavelength was the fact that it does not correspond to any CCO absorption band. At this wavelength, there is a large water absorption band, making 980-nm photons more likely to produce tissue heating than photochemical effects. The fact that reported results for 980-nm-based LLLT are mixed also leads us to choose this wavelength. The literature presents conflicting results in wound healing,<sup>35,36</sup> positive effects on neuropathic pain relief,<sup>37</sup> and no effects on traumatic brain injury.<sup>38</sup> Published data on the effectiveness of 980 nm in the treatment of skeletal muscle inflammation are very scarce, a fact that also prompted us to use this wavelength.

The laser beam profile and shape were measured with a BeamStar PCI-PAL 100345 beam profiler (Ophir, Jerusalem, Israel) at a plane corresponding to the animal leg. The 830-nm beam presented an elliptical shape, with horizontal and vertical profiles whose correlation coefficients to Gaussian shape were 78.5% and 90.7%, respectively. Profiles widths at  $1/e^2$  were  $9.74 \pm 0.003$  mm, for the horizontal profile, and  $8.31 \pm 0.001$  mm, for the vertical profile, resulting in a beam spot size at target of  $0.80 \text{ cm}^2$ . The 830-nm beam two-dimensional (2-D) and three-dimensional (3-D) shapes are shown in Fig. 2, along with its horizontal and vertical profiles.

The 980-nm laser also presented an elliptical shape. The correlation coefficients between the horizontal and vertical profiles and a Gaussian profile were 80.1% and 82.2%, respectively. The measured profiles widths at  $1/e^2$  were  $9.26 \pm 0.001$  mm, for the horizontal profile, and  $7.42 \pm 0.001$  mm, for the vertical profile, resulting in a beam spot size at target of  $0.69 \text{ cm}^2$ . Figure 3 presents the 2-D and 3-D shapes and horizontal and vertical profiles for the 980-nm laser beam.

These measurements required the use of neutral density (ND) filters to prevent CCD saturation. Speckle is not evident in the actual treatment conditions. The large ring patterns visible in Figs. 2 and 3 probably result from interference effects due to reflections on the ND filters. The small circular patterns are most probably due to dust on the filters.

The animals were randomly divided into one control group ( $n = 10$ ) and 15 treatment groups ( $n = 5$ ), defined by different irradiation and treatment parameters. Ten groups concern CW irradiation (radiant powers between 10 and 50 mW, at 10 mW steps, for both 830 and 980 nm), while the remaining five groups underwent PW irradiation (Peak power: 50 mW, Average Power: 40 mW, Duty cycle: 80%, frequencies: 5, 25, 50, 100, and 200 Hz).

LLLT was applied daily, perpendicular to the muscle's surface. Exposure time was always constant and equal to 3 min. Average energy per application was 0 J (control group), 1.8, 3.6, 5.4, 7.2, and 9.0 J, in the CW groups, and 7.2 J in the

PW groups. Laser treatment was applied daily, under artificial light, at the same time of the day (9:00 a.m.) for 5 days (from day 1 to day 5) directly to shaved skin by transcutaneous application. Beam laser incidence was kept perpendicular to the irradiation area. Only one spot was irradiated. During irradiation, animals were anesthetized with a mixture of isoflurane (2.5%) and oxygen (97.5%) at a flow of 1.5 l/min. Control rats were also anesthetized to ensure standardization, but did not receive laser treatment.

Regarding the used irradiation parameters, the total energy was selected according to the World Association for Laser Therapy (WALT) recommended treatment doses for LLLT, which vary between 4 and 16 J. The radiant powers were selected in order to obtain irradiances in the higher half of the common range of values used for stimulation and healing ( $5$  to  $50 \text{ mW/cm}^2$ )<sup>39</sup> and are similar to those reported for modulation of cytokines expression in skeletal muscle following acute injury.<sup>10,32,40</sup>

For PW repetition rates, due to the lack of reference values for the treatment of skeletal muscle inflammation, we choose to use values similar to those reported for pain reduction, since pain relief seems to be obtained by the anti-inflammatory action of LLLT.

It is important to stress that we performed the experiments sequentially. First, we did the CW treatments. The PW measurements were done afterward and using only the wavelength and average power that yielded the best results with CW irradiation. This way we complied with the reduction principle on animal experimentation, minimizing the number of animals used.

## 2.4 Blood Sampling

Blood was collected on days 0 (5 h after inflammation induction), 3, and 6 (before animal sacrifice), always at 2:00 p.m. A blood volume of 1 ml was taken through the jugular vein. This is in accordance with the blood sample limit of 8 ml/kg each 14 days.<sup>41,42</sup> During blood collection, the animals were anesthetized in the conditions previously described.

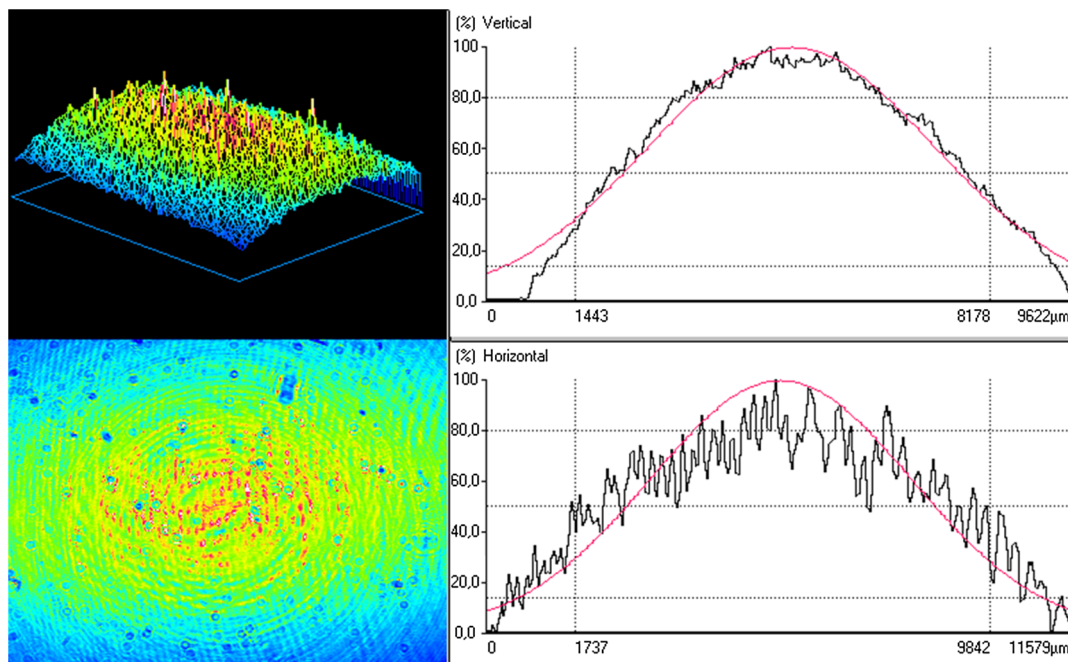
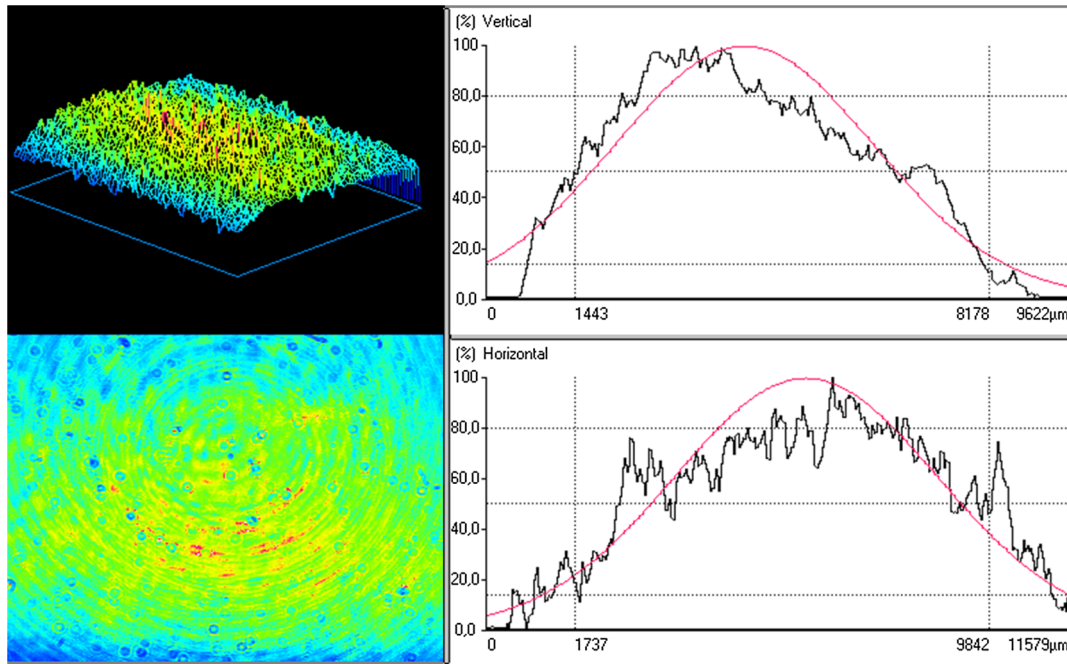


Fig. 2 Beam shape and profile for the 830-nm laser beam. The smooth line indicates a Gaussian profile.



**Fig. 3** Beam shape and profile for the 980-nm laser beam. The smooth line indicates a Gaussian profile.

All blood samples were placed in BD Vacutainer Plastic SST II Advance tubes (BD, Franklin Lakes, New Jersey, USA) for subsequent centrifuging (15 min., 3500 rpm at 4°C). The serum was removed and the samples were stored at -20°C. The followed work schedule is summarized in Fig. 4.

### 2.5 ELISA Analysis

ELISA serum analysis was done using Peprotech ELISA Kits (PeprTech EC Ltd., London, United Kingdom) for quantifying TNF- $\alpha$ , IL-1 $\beta$ , IL-2, and IL-6 cytokines. We used a BioTek Synergy HT microplate reader (BioTek Instruments, Inc., Winooski, Vermont, USA) at 405 nm, with a wavelength correction set at 650 nm. The plate was monitored at 5-min intervals for 45 min.<sup>43</sup> The samples' concentrations were calculated by interpolation of the regression curve using the Gen 5 HT software (BioTek Instruments, Inc., Winooski, Vermont, USA).

Comparisons between different cytokines concentrations and concentrations decrease were done using analysis of variance (ANOVA) with post hoc between-group comparisons by the Tukey test.<sup>44</sup> A significance level of 0.05 was considered in all cases.

### 2.6 Muscle Sample Preparation and Examination

Rats were killed on day 6 for histological analysis of muscle. The animals were anesthetized before blood sampling and cervical dislocation.

The gastrocnemius muscle was rapidly removed from the injured leg, snap frozen in cryopreservation resin, and stored at

-80°C until analysis. The surgical procedure took less than 15 min.

5- $\mu$ m thick cuts were made transversely to the muscular fibers with a glass knife using a Leica Microsystems CM3350S cryostat (Leica Microsystems, Wetzlar, Germany). After dewaxing and hydration, the samples were colored with hematoxylin-eosin and fixed with DPX mountant for microscopy in order to observe the hematoma area and other visible changes.

The cross sections were observed with a Motic AE 31 inverted microscope (Motic Ltd. Hong-Kong, China), using 10X, 20X, and 40X objectives. The muscles images were captured using a high resolution camera Motic Moticam 2. The most representative cuts were selected. Hematoma areas were identified by visual inspection.

The number of inflammatory cells was compared using the images obtained with the 20X objective. Cells were counted using an unbiased counting frame.<sup>45</sup> Comparisons between different rats were analyzed using ANOVA procedure, with post hoc between-group comparisons through the Tukey test, with a significance level of 0.05. For each animal, 10 images were used for inflammatory cell counting.

### 2.7 Monte Carlo Simulation of Light Transport in Tissue

The expected dose in muscle tissue was evaluated through computer Monte Carlo (MC) simulation of light transport in a heterogeneous medium. MC simulations were done with the

	Day 0	Day 1	Day 2	Day 3	Day 4	Day 5	Day 6
Since 9:00 a.m.	Inflammation induction	Treatment	Treatment	Treatment	Treatment	Treatment	
Since 2:00 p.m.	Blood sampling			Blood sampling			Blood sampling sacrifice

**Fig. 4** Experimental work schedule.

**Table 1** Optical parameters for the tissue model used in Monte Carlo simulation of light transport.

Layer	$\mu_a$ (cm <sup>-1</sup> )		$\mu_s$ (cm <sup>-1</sup> )		g	
	830 nm	980 nm	830 nm	980 nm	830 nm	980 nm
Skin	0.17	0.35	74.49	72.05	0.82	0.84
Muscle	1.15	1.15	91.82	89.79	0.88	0.89

mcxyz.c code developed and made available by Jacques et al.<sup>46</sup> We used a two-layer tissue model: skin (thickness: 2.1 mm) and muscle. The laser beam was modeled as a Gaussian beam with a diameter of 8 mm at the  $1/e^2$  contour. The optical parameters were obtained from published research work<sup>47,48</sup> and are summarized in Table 1.

### 3 Results

#### 3.1 Cytokines Measurement Through ELISA: Continuous-Wave Irradiation

Figure 5 shows the decrease in cytokines concentration at day 6, expressed as percentage of the concentration at day 0, for CW irradiation at 830 and 980 nm. For each group, we tested whether or not the measured cytokines relative concentration decrease was different from those measured for the control group. Significantly different concentration decreases are identified. As Fig. 5 shows, the treatment effect was higher for irradiation at 830 nm. For this wavelength, the TNF- $\alpha$  concentration

decrease was significantly higher for almost all treated groups, the exception being the 50-mW group. This higher TNF- $\alpha$  decrease could be already observed at day 3 for the 20, 30, and 40 mW groups. The highest variation between days 0 and 6 was found in the 30-mW group and was statistically higher than those observed in the other treatment groups. The lower effectiveness of the 930-nm irradiation is revealed by the lower number of treatment groups that achieved a statistically higher relative TNF- $\alpha$  decrease than that measured for the control group. At day 6, LLLT was only effective for the 30 and 40-mW groups, with no statistically significant difference between them. When comparing between treated groups at 830 and 980 nm with the same radiant power and energy dose, we find that TNF- $\alpha$  concentration decrease is higher at 830 nm for the 20, 30, and 40 mW groups.

IL-1 $\beta$  measurements at day 6 show higher relative concentration decreases for the 30, 40, and 50 mW groups when compared with controls for both irradiation wavelengths. This could be already clearly observed at day 3 for the 40 and 50 mW

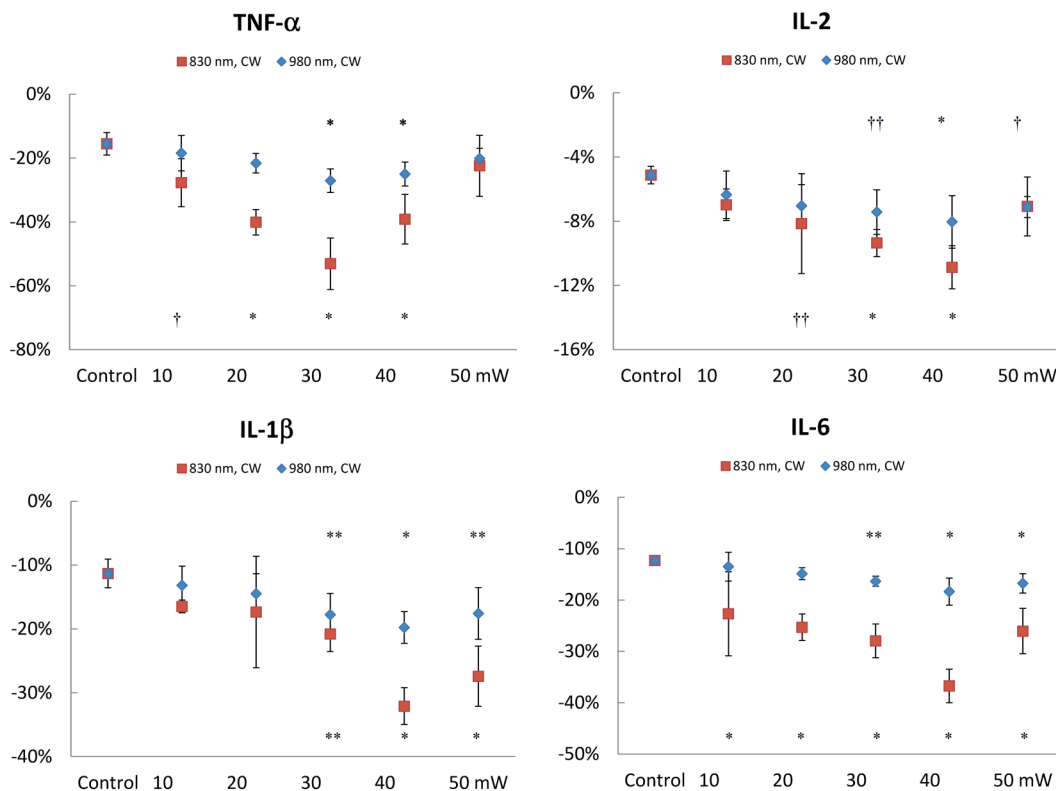


**Fig. 5** Cytokine concentration decrease for CW irradiation at 830 and 980 nm, at day 6. Values are expressed as percentage of the concentration at day 0. Error bars indicate standard deviations (SD  $\pm$ ). Significant difference in relative cytokines concentration decrease for comparisons with control group: \*  $p < 0.001$ ; \*\*  $p < 0.008$ ; †  $p < 0.05$ ; ††  $p < 0.015$ .

groups at 830 nm ( $p < 0.001$ ), and for the 40-mW group at 980 nm ( $p < 0.001$ ). The highest variation between days 0 and 6 occurred in the 40-mW group for both wavelengths. Animals treated with the 830-nm laser show a statistically higher IL-1 $\beta$  concentration decrease in the 40 mW groups than those measured in the 10, 20, and 30 mW groups ( $p < 0.002$ ). The concentration decrease was lower for animals treated at 980 nm. Comparison between groups treated at 830 and 980 nm with equal radiant power yielded a higher decrease at 830 nm for the 40 ( $p = 0.002$ ) and 50 mW ( $p = 0.016$ ) groups.

IL-2 measurements at day 6 show higher concentration decreases for the 20, 30, and 40 mW groups at 830 nm, and for the 30, 40, and 50 mW groups at 980 nm. A significant decrease at day 3 was observed only in the animals treated with the 830-nm laser at 40 mW ( $p = 0.002$ , when compared with controls). Once again, the highest variation between days 0 and 6 occurred in the 40-mW group. Although this took place for both wavelengths, we only found differences when comparing the 10 and the 50 mW groups and just for the animals treated with the 830-nm laser. At 980 nm, no differences were found between treatment groups at day 6. The comparison between LLLT groups with the same radiant power at 830 and 980 nm yielded no differences.

The results at day 6 for IL-6 show higher concentration decreases for all treatment groups ( $p < 0.001$ ) at 830 nm and for the 30, 40, and 50 mW groups at 980 nm. At day 3, it was already possible to observe significant decreases in the IL-6 concentration in the 30, 40, and 50 mW groups treated with the 830-nm laser. No significant IL-6 concentration decreases were observed at day 3 in the animals treated with the 980-nm laser.

The highest concentration variation between days 0 and 6 occurred again at 40 mW for both wavelengths. For LLLT with 830 nm, the IL-6 decrease at day 6 in the 40-mW group is significantly higher than those obtained for the other treatment groups. This is also true at day 3, except when compared to the animals irradiated at 50 mW. For animals treated with the 980-nm laser, differences between the 40 mW and the other treatment groups were only found when compared to the 10 and 20 mW at day 6. The comparison between equivalent LLLT groups at 830 and 980 nm produced significant differences for all compared groups, being highly significant ( $p < 0.001$ ) for the 30 and 40 mW groups. For the 40 mW groups, this highly significant difference appears at day 3.

### 3.2 Cytokines Measurement Through ELISA: Pulsed-Wave Irradiation

Figure 6 shows the decrease in cytokines concentration at day 6, expressed as percentage of the concentration value at day 0 for 830-nm PW irradiation with constant average and peak powers at different frequencies. Concentration decreases significantly different than those observed for the control group are identified. As Fig. 6 shows, the treatment effect was higher for irradiation at frequencies higher than 50 Hz. The TNF- $\alpha$  concentration decrease was significantly higher for the 50, 100, and 200 Hz groups. This higher TNF- $\alpha$  decrease could be already observed at day 3, mainly for the 100 Hz group ( $p = 0.001$ ) but also for the 200 Hz group ( $p = 0.010$ ). The highest variation from days 0 to 6 was observed in the 100-Hz group. However, it was not statistically different from those observed for the 50 and 200 Hz groups.

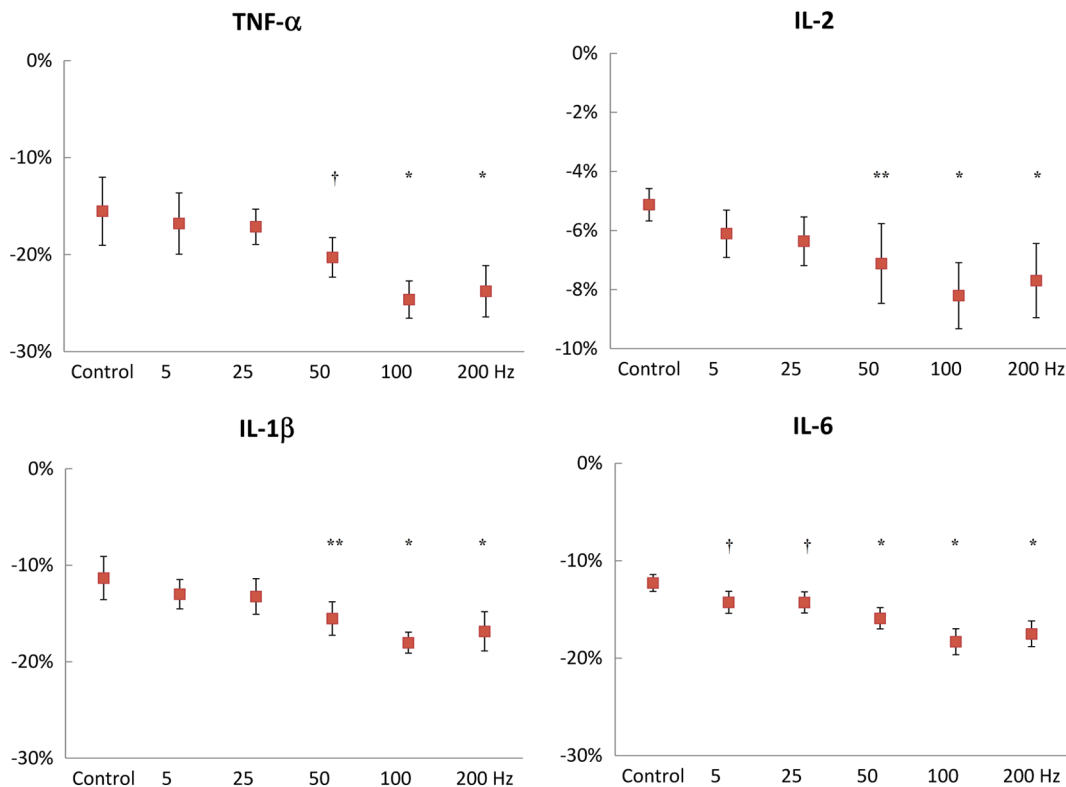


**Fig. 6** Cytokine concentration decrease for PW irradiation at 830 nm, at day 6. Values are expressed as percentage of the concentration at day 0. Error bars indicate standard deviations (SD  $\pm$ ). Significant difference in relative cytokines concentration decrease for comparisons with control group: \*  $p < 0.001$ ; \*\*  $p < 0.008$ ; †  $p < 0.05$ .

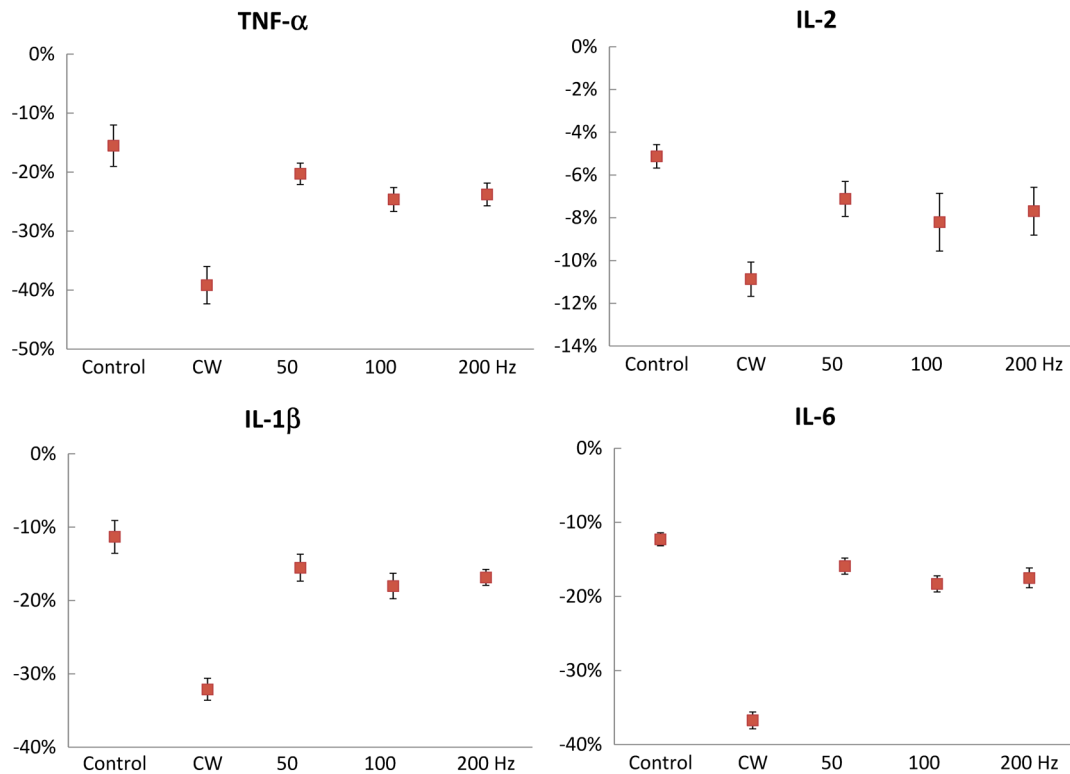


**Fig. 7** Comparison between cytokine concentration decrease for CW and PW irradiations at 830 nm at day 6. Values are expressed as percentage of the concentration at day 0. Error bars indicate standard deviations (SD  $\pm$ ).

The IL-1 $\beta$  and IL-2 measurements show a similar behavior to the TNF- $\alpha$  measurements. Significant differences were found at day 6 for the 50, 100, and 200 Hz groups when compared to controls. However, at day 3, differences were only found in IL-2 measurements for 100 and 200 Hz. The highest variation between days 0 and 6 was measured for the 100 Hz but, again, with no statistically differences from the variations observed in the 50 and 200 Hz groups.

The IL-6 cytokine concentration decrease at day 6 is significantly higher for all treatment groups when compared with the control group. This was already true at day 3 for the higher frequencies groups (50, 100, and 200 Hz). The highest variation between days 0 and 6 occurred again for the 100-Hz group. This time, the concentration decrease observed for 100 Hz is statistically different from the one measured for 50 Hz, but not from the value obtained in the 200-Hz group.

Figure 7 compares the decrease in cytokines concentration at day 6 between PW irradiation at 50, 100, and 200 Hz and CW irradiation at 40 mW. All values are for treatment at 830 nm. It is easily seen that the cytokines relative concentration decrease is larger for CW irradiation. The differences are statistically significant, with all but one  $p$  value smaller than 0.001 ( $p = 0.005$  for IL-2, CW versus 100 Hz). At day 3, there are already statistically significant differences between the PW group and the CW irradiated animals for the variation of TNF- $\alpha$ , IL-1 $\beta$ , and IL-6 cytokines. For IL-2, no differences were found at day 3 between the treatment groups.

### 3.3 Inflammatory Cells Counting

Table 2 shows the results from inflammatory cell counting on microscopy images of 5- $\mu$ m thick cuts from the gastrocnemius

muscle of control and CW treated animals. Figure 8 shows the representative images of gastrocnemius muscle cuts. For each animal, the counting value is the average of measurements done in 10 slides. The values presented are the average for all animals in a given group. Significant differences ( $p < 0.001$ ) were found between the control and all treatment groups for both irradiation wavelengths. The lowest counts of inflammatory cells were obtained at 40 mW. For the 830-nm laser, there are differences between the cell counting at 40 mW and at 10, 20, and 30 mW. With the 980-nm laser, the differences exist only when compared to the 10 and 20 mW groups.

The images from animals irradiated with the 830-nm laser present less inflammatory cells when compared with the muscle cuts from animals treated at 980 nm. However, as Table 2 shows, the differences are not statistically significant for the level of confidence used.

**Table 2** Inflammatory cell counting in images of the gastrocnemius muscle of control and CW treated animals. Values are average  $\pm$  SD.

Group	830-nm laser	980-nm laser	$p$ (830 versus 980 nm)
Control	17.76 $\pm$ 0.79	17.76 $\pm$ 0.79	
10 mW	14.30 $\pm$ 1.59	14.88 $\pm$ 1.59	0.97
20 mW	13.24 $\pm$ 1.66	14.06 $\pm$ 1.42	0.79
30 mW	12.78 $\pm$ 1.84	13.08 $\pm$ 1.54	1.00
40 mW	10.84 $\pm$ 1.57	12.29 $\pm$ 1.96	0.09
50 mW	12.08 $\pm$ 2.06	13.02 $\pm$ 1.39	0.63



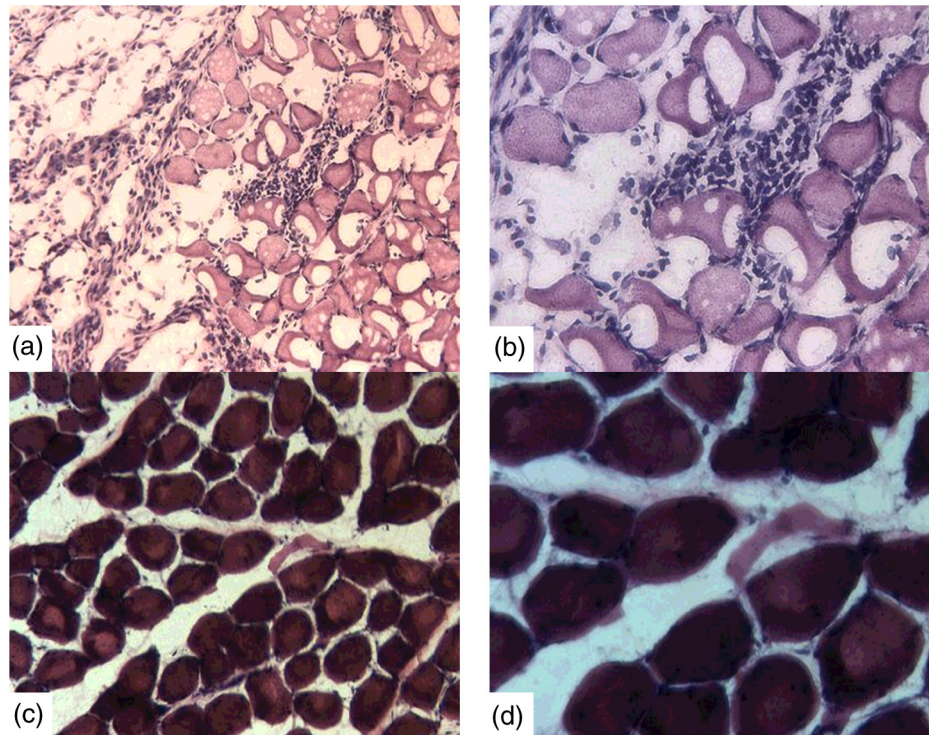


**Fig. 8** Images from gastrocnemius muscle cuts. Control rat: (a) 20 $\times$ ; (b) 40 $\times$ ; rat from 40-mW group: (c) 20 $\times$ ; (d) 40 $\times$ . In the control rat without treatment, it is possible to observe an infiltration of inflammatory cells. The treated rat shows an improved condition, although still presents inflammatory cells.

Table 3 presents the inflammatory cell count for PW irradiation and CW 40 mW at 830 nm. Significant differences were found between the control group and each of the CW, 50, 100, and 200 Hz groups ( $p < 0.001$ ). The number of inflammatory cells for the CW is also significantly lower than for every PW irradiation group ( $p < 0.001$ ). For PW irradiation, no significant differences can be found among the 50, 100, and 200 Hz groups.

### 3.4 Simulation of Light Transport in Tissue

Figure 9 shows the irradiance ( $\text{W}/\text{cm}^2/\text{W}$  delivered) distribution in the tissue model for irradiation at 830 and 980 nm. It also includes the normalized irradiance as a function of tissue depth. The results show that there are no differences in the depth

**Table 3** Inflammatory cell counting in images of the gastrocnemius muscle of control and 40 mW (average power), 830-nm treated animals (CW and PW). Values are average  $\pm$  SD.

Group	Cell counting
Control	17.76 $\pm$ 0.79
CW	10.84 $\pm$ 1.57
5 Hz	16.62 $\pm$ 1.61
25 Hz	16.56 $\pm$ 1.92
50 Hz	15.64 $\pm$ 1.74
100 Hz	14.66 $\pm$ 1.25
200 Hz	15.18 $\pm$ 1.14

irradiation profiles between 830 and 980 nm. Therefore, differences of treatment effects between those wavelengths are not due to irradiance differences in the target area.

## 4 Discussions and Conclusions

Our objective was to evaluate the effect of different LLLT irradiation parameters, namely radiant power, wavelength, and continuous versus pulsed illumination, on the inflammation phase of skeletal muscle injury. A quantitative evaluation of LLLT effects was achieved by measuring the concentration of inflammatory cytokines (TNF- $\alpha$ , IL-1 $\beta$ , IL-2, and IL-6) in the systemic blood. Tumor necrosis factor (TNF)- $\alpha$  and interleukin (IL)-1 are two key cytokines, produced in response to trauma, that promote inflammatory responses, including the recruitment of immune cells to the injured area. IL-6 is also a proinflammatory cytokine that is responsible, with TNF- $\alpha$  and IL-1, for increasing the liver synthesis of most acute-phase proteins. IL-2 has both pro- and anti-inflammatory roles. It is a potent inducer of T-cell proliferation, but also has regulatory roles, namely in the development and function of regulatory T cells. Thus, IL-2 contributes both to the induction and the end of acute inflammatory responses.

Cytokines have been used to quantify LLLT effects in treating inflammation. Piva et al.<sup>25</sup> reviewed the effect of LLLT on the initial stages of tissue repair, reporting several studies where LLLT decreases the expression of TNF- $\alpha$ , IL-1 $\beta$ , and IL-6. In what concerns skeletal muscle injury, one of the reviewed studies shows that TNF- $\alpha$ , IL-1 $\beta$ , and IL-6 mRNA expression is decreased when using LLLT to treat inflammation of the subplantar muscle of a rat paw.<sup>49</sup> LLLT was also able to reduce the TNF- $\alpha$  and IL-1 $\beta$  concentrations in rat tibialis anterior muscle after cryolesion.<sup>9,10</sup> Although in most LLLT studies, cytokines concentration is measured in a muscle sample homogenate, we choose to measure the cytokines concentration in

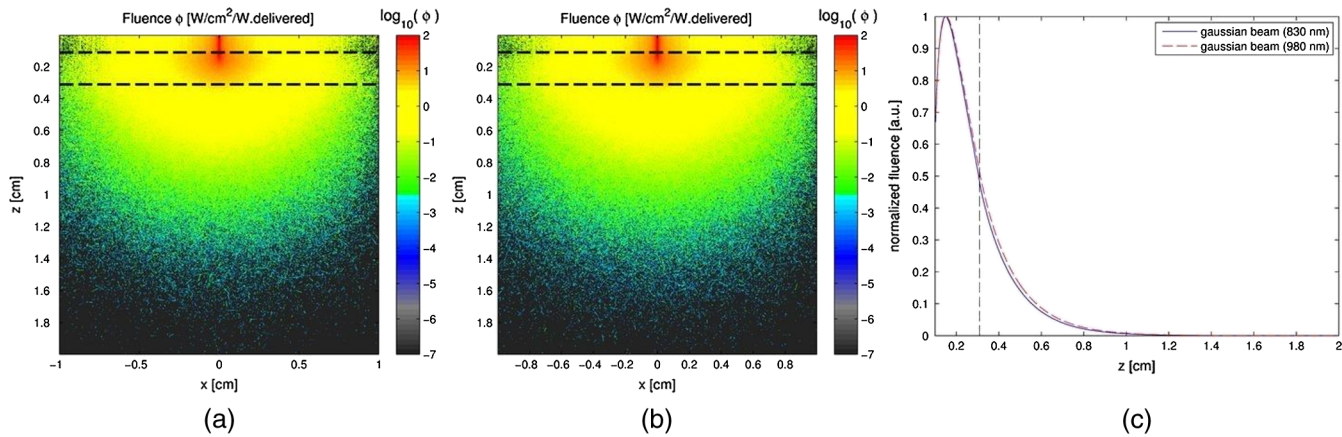


**Fig. 9** Irradiance ( $\text{W}/\text{cm}^2/\text{W}$  delivered) distribution in the tissue, for irradiation at 830 nm (a) and 980 nm (b) and normalized irradiance profile as a function of tissue depth (c). In (a) and (b), the dashed top line identifies the air-skin interface. The dashed bottom line corresponds to the skin-muscle interface. In (c) the dashed line corresponds to the skin-muscle interface.

systemic blood serum. This allows sampling during treatment without sacrificing the animals. Moreover, this quantification method can be applied to human studies. Zhevago and Samoilova<sup>50</sup> have previously shown in humans, that transcutaneous irradiation with visible and infrared light modulates cytokines concentration on peripheral systemic blood, namely by decreasing the concentration of  $\text{TNF-}\alpha$  and IL-6.

Our results show treatment effects, particularly for irradiation with the 830-nm laser. At day 6, the concentration of all measured proinflammatory cytokines in the 30 and 40 mW groups was significantly lower than for the control group. IL-6 concentration was reduced for all treatment groups and  $\text{TNF-}\alpha$  for all but the 50-mW group. The number of inflammatory cells in muscle tissue samples was also significantly lower in all treatment groups when compared to the control animals.

The best results were obtained with a radiant power of 40 mW at 830 nm. This was the only group of animals where the concentration of all measured cytokines was already significantly lower at day 3 when compared to the control group. The lowest counts of inflammatory cells were also obtained in the 40-mW group. As Fig. 1 clearly shows, the treatment effects decrease both for radiant powers below and above 40 mW. This behavior may suggest a biphasic dose response.<sup>39,51</sup> We varied the delivered energy dose ( $\text{J}/\text{cm}^2$ ) per application by adjusting the laser power while keeping the irradiation time constant at 3 min. For the used radiant powers and the measured beam areas at skin ( $0.80 \text{ cm}^2$  for 830 nm;  $0.69 \text{ cm}^2$  for 980 nm), this amounts to a dose range between 2.25 and  $13.0 \text{ J}/\text{cm}^2$ , with the peak effect at  $9 - 10 \text{ J}/\text{cm}^2$ . There are some published studies reporting biphasic responses for comparable energy doses. In one study with macrophage cell lines irradiated at 820 nm, Bolton et al.<sup>52</sup> observed cell proliferation from 2.4 to  $9.6 \text{ J}/\text{cm}^2$ , finding a maximum at  $7.2 \text{ J}/\text{cm}^2$ . An animal study<sup>53</sup> on mouse pleurisy induced by carrageenan treated with a 650-nm laser at three dose values (3, 7.5, and  $15 \text{ J}/\text{cm}^2$ ), found the largest inflammatory cell migration reduction at  $7.5 \text{ J}/\text{cm}^2$ . A final conclusion for the biphasic response behavior requires additional measurements for doses greater than  $13.0 \text{ J}/\text{cm}^2$  to verify if the LLLT effect still decreases for those doses.

LLLT treatment was less effective at 980 nm. The light transport in a two-layer tissue model was simulated to assess if the lower effect observed with irradiation at 980 nm was due

to lower muscle irradiance for that laser wavelength. Our MC simulations showed that the normalized irradiance at the muscle is equal for 830 and 980 nm. In fact, although skin absorption is higher for 980-nm, scattering in the skin is higher at 830 nm. The combination of the two processes seems to result in very similar profiles for the dependence of irradiance with tissue depth.

The lower treatment effect at 980 nm seems to result from specific absorption properties of the chromophores mediating LLLT effects. The probable photo acceptor in mammalian cells for visible and near-infrared (NIR) light is CCO, the terminal electron acceptor of the mitochondrial electron transport chain in eukaryotic cells.<sup>34</sup> It is known that the action spectrum of CCO has a peak at 825 nm, and is thought to be due to the relatively oxidized  $\text{Cu}_A$  chromophores.<sup>34</sup> Specific extinction spectrum of oxidized and reduced CCO from bovine heart tissue shows larger extinction coefficients at 830 nm when compared with values measured at 980 nm (1.7 times higher for oxidized CCO and 1.2 times higher for reduced CCO).<sup>54</sup> This difference may justify the larger treatment effect observed at 830 nm.

The irradiance values on the central region of the irradiated tissue volume raise the issue of whether thermal effects play a role on the experiments. In fact, we planned our experiments considering *a priori* that thermal effects were not significant. This was based on measurements in humans reported by Joensen et al.,<sup>55</sup> using a 810-nm laser with an output power of 200 mW, spot size of  $0.0314 \text{ cm}^2$  and power density of  $6.37 \text{ W}/\text{cm}^2$ , values that produce local irradiances much higher than those we used. The measurements showed small thermal effects in light skin (a condition closer to our experiments with albino rats), with temperature increases ranging from  $0.38^\circ\text{C}$  to  $1.58^\circ\text{C}$ , for 9 J of delivered energy.

The MC simulations of light propagation allow us to do a simple evaluation of possible thermal effects by calculating the average irradiance in skin and muscle and the temperature increase in these tissues. Simulation data show that thermal effects are only relevant in the central region of the beam, taken as the region of the beam profile where intensity is higher than 80% of the peak intensity. The temperature increase in the muscle is not significant. The calculated value, without considering the effects of thermal diffusion or blood convection, was close to  $1^\circ\text{C}$ . The temperature increase is larger in the skin since

it absorbs more light, and this is more pronounced for 980-nm irradiation. This further suggests that thermal effects are not responsible for the observed treatment effects, which are more pronounced for 830 nm.

For the animals treated with PW irradiation, cytokines reduction was only significant for the higher frequencies (50, 100, and 200 Hz), although cytokines concentration decrease was much lower than the one obtained for CW irradiation with the same radiant power. The reduction in inflammatory cells was also significantly lower with PW irradiation than the one measured for CW illumination. These results suggest that pulsed irradiation is less effective than CW irradiation with the same average power in the reduction of the inflammatory phase of skeletal muscle injury.

There is published evidence that pulsed irradiation produces different effects than CW irradiation. Hashmi et al. recently reviewed the effects of pulsing in LLLT,<sup>27</sup> reporting nine studies comparing CW and PW irradiations, none of them on muscle inflammation. Of those, seven found beneficial effects from pulsed irradiation with only one study finding a higher treatment effect with CW irradiation, although by a minimal margin. Biological reasons are usually proposed for the increased efficiency of PW irradiation, namely modulation of ion channels kinetics in the milliseconds time range or promotion of multiple nitric oxide photodissociation events from a protein binding site.<sup>27</sup>

In our experiments, the duty cycle was 80%, resulting in a peak power 20% higher than the CW radiant power. Therefore, during pulse exposure, the irradiance at muscle tissue is 20% higher than during CW irradiation, although the radiant exposure is kept equal. If we examine the existence of irradiance effects on LLLT, which are clearly suggested by the observed biphasic dose responses that imply a lack of compliance to the Bunsen–Roscoe rule of reciprocity,<sup>51</sup> a direct comparison between CW and PW irradiations with the same average power may be partially hampered by such effects. The higher irradiance stimulus occurring with PW irradiation may inhibit to some degree the LLLT action, resulting in a treatment effect lower than that observed for CW irradiation at 40 mW. This is supported by the results obtained with CW irradiation at 50 mW.

It is relevant to note that our data yield mixed results when we compare CW irradiation at 50 mW and PW irradiation at the higher frequencies. PW irradiation was significantly more effective than CW irradiation for reducing TNF- $\alpha$  concentration, as effective as CW irradiation for decreasing IL-2 concentration, and less effective than CW irradiation concerning IL-1 $\beta$  and IL-6. CW irradiation at 50 mW also resulted in a lower count of inflammatory cells than PW irradiation. A new set of PW measurements using a peak power of 40 mW could be useful to properly address the impact of irradiance effects.

None of the published studies comparing CW and PW irradiations deal with skeletal muscle inflammation. Our data suggest that CW irradiation is more effective in the treatment of the inflammation phase of skeletal muscle injury than PW irradiation with the same radiant exposure. However, irradiance effects may hinder this conclusion. Therefore, further investigations are required.

PW irradiation only produced treatment effects for higher frequencies (50, 100, and 200 Hz). Once again, we could not find any study comparing pulse repetition rates in the treatment of muscle inflammation. An *in vitro* study,<sup>56</sup> designed to evaluate if pulsed light can overcome the filtering effects of melanin exposed human HEP-2 cells to 670-nm CW or PW light at

several repetition rates (6, 18, 36, 100, and 600 Hz) through melanin filters. The authors found that cell proliferation was increased in the groups treated with PW irradiation, with maximal effects at 100 Hz, suggesting that penetration of PW light through tissues with high melanin content depends on pulse frequency. However, this effect does not play a role in our experiments since we used albino Wistar rats. Multiple nitric oxide photodissociation events from a protein binding site are another mechanism proposed for explaining PW effects in LLLT.<sup>27</sup> Although this mechanism may play a significant role in irradiation with pulsed light in the red region, NIR wavelengths are absorbed by a part of the CCO not involved in NO binding,<sup>57</sup> suggesting that photodissociation is not responsible for the positive effects of PW for NIR irradiation.

The observed larger effects of PW irradiation for 50, 100, and 200 Hz frequencies suggest the existence in this frequency range of some fundamental frequency in involved biological systems or some process with a time scale of milliseconds. The most obvious time constant is the thermal relaxation time of blood vessels, which again raises the question of the involvement of thermal effects.

Considering the thermal relaxation time of an infinite cylinder, we find that time constants between 5 and 20 ms can be associated with thermal relaxation of vessels with diameters between 100 and 200  $\mu\text{m}$ . These diameters are larger than those found in dermis capillaries.<sup>58</sup> We simulated the thermal behavior of blood vessels for vessel diameters between 50 and 220  $\mu\text{m}$  and considering the frequencies used in our PW measurements. For that purpose, we used the values of average irradiance for skin and muscle obtained through our MC simulations and computed the thermal behavior following a methodology identical to that used by Stuart Nelson et al.<sup>59</sup> For vessels located within the muscle tissue, the temperature increase is always negligible (lower than 0.03°C). Significant temperature effects may occur for skin blood vessels with diameters larger than 70  $\mu\text{m}$ . However, these vessel diameters are rarely found in normal dermis. It is also important to note that temperature effects are more significant for low frequencies, which were the frequencies that resulted in lower treatment effects. For these reasons, it seems very unlikely that the frequency dependence of the measurements is due to the thermal relaxation of blood vessels.

Currently, the more accepted cellular level mechanism for LLLT is the absorption radiation by components of the cellular respiratory chain. Therefore, we looked at this chain for processes with time constants in the range of milliseconds. Starting from fully oxidized CCO, the electronic transfer rate from cytochrome *a* to cytochrome *a*<sub>3</sub> occurs in the millisecond time range, even with large reductant concentrations.<sup>60</sup> Simulations done by Brunori et al.<sup>60</sup> resulted in forward and reverse rate constants for the electronic transfer from cytochrome *a* to cytochrome *a*<sub>3</sub> equal to 25 and 125 s<sup>-1</sup>, respectively. Karu<sup>34</sup> suggests that irradiation intensifies the cytochrome *a* to cytochrome *a*<sub>3</sub> electron transfer stage, since this is the rate-limiting step in the whole electron transfer within the CCO, making more electrons available for the reduction of dioxygen. Taking its rate constants, it is possible to suggest that PW irradiation with frequencies comparable to those rates will be more effective in intensifying the cytochrome *a* to cytochrome *a*<sub>3</sub> electron transfer when compared with irradiation at lower frequencies.

In conclusion, we were able to quantify the effect of LLLT on the treatment of inflammation induced in the gastrocnemius

muscle of Wistar rats by measuring the concentration of proinflammatory cytokines in the systemic blood, a method that allows following the treatment effect without sacrificing animals. The results showed that CW irradiation at 830 nm produced the largest treatment effects, a result in accordance with the action spectrum of CCO. Best results were obtained with an irradiation power of 40 mW, with the data suggesting a biphasic dose response. This suggestion requires further confirmation through experiments using higher radiant powers. PW irradiation at 830 nm and 40-mW average power was only effective for the tested frequencies equal to or higher than 50 Hz. This result might be related to the rate constants of the CCO internal electron transfer stage between cytochrome *a* and cytochrome *a*<sub>3</sub>.

LLLT have been used since 1960s to improve the healing of different soft-tissue pathologies and to reduce the perception of both nociceptive and neuropathic pain. Histological studies report increased microvascularization and a positive influence on fibroblast proliferation, collagen synthesis, and tissue regeneration. In rehabilitation medicine, LLLT was introduced as a noninvasive and safe treatment, but its efficacy is still controversial because several clinical trials have reported its ineffectiveness to treat pain and inflammation in musculoskeletal disorders.

Researchers and clinicians should consistently report the characteristics of the device, the irradiation parameters, and the treatment procedures. If we are able to quantify the effect of LLLT on the relief of pain and inflammation using a rigorous methodology, we can choose the best therapeutic window, increasing the efficiency and credibility of this physical agent. This work is intended to be a contribution toward this goal. Its potential clinical impact result lies in the methodology used to quantify inflammation relief and on the identification of the best irradiation and treatment parameters for achieving that relief.

### Acknowledgments

This study was supported in part by the Fundação para a Ciência e a Tecnologia (FCT) under program COMPETE FCOMP/01-0124-FEDER-022709 and by Erasmus Mundus EADIC Scholarships. Thanks to "Industrias Mantineo," Mendoza, Argentina, for building the inflammation induction equipment. We also thank the help of Mr. António Correia, MSc with the Monte Carlo simulations.

### References

1. J. D. Carroll, "Photomedicine and LLLT literature watch," *Photomed. Laser Surg.* **27**(4), 689–90 (2009).
2. C. Antipa et al., "Our clinical experience in low-energy laser medical treatments," *Opt. Eng.* **35**(5), 1367–1371 (1996).
3. R. A. B. Lopes-Martins et al., "Low level laser therapy [LLLT] in inflammatory and rheumatic diseases: a review of therapeutic mechanisms," *Curr. Rheumatol. Rev.* **3**(2), 147–154 (2007).
4. K. Nomura, M. Yamaguchi, and Y. Abiko, "Inhibition of interleukin-1 beta production and gene expression in human gingival fibroblasts by low-energy laser irradiation," *Lasers Med. Sci.* **16**(3), 218–223 (2001).
5. H. Chung et al., "The nuts and bolts of low-level laser (light) therapy," *Ann. Biomed. Eng.* **40**(2), 516–533 (2012).
6. A. C. M. Rennó et al., "Comparative effects of low-intensity pulsed ultrasound and low-level laser therapy on injured skeletal muscle," *Photomed. Laser Surg.* **29**(1), 5–10 (2011).
7. G. Shefer et al., "Low-energy laser irradiation promotes the survival and cell cycle entry of skeletal muscle satellite cells," *J. Cell Sci.* **115**(Pt 7), 1461–1469 (2002).
8. R. Albertini et al., "Effects of different protocol doses of low power gallium-aluminum-arsenate (Ga-Al-As) laser radiation (650 nm) on carrageenan induced rat paw oedema," *J. Photochem. Photobiol. B* **74**(2–3), 101–107 (2004).
9. L. Assis et al., "Low-level laser therapy (808 nm) reduces inflammatory response and oxidative stress in rat tibialis anterior muscle after cryo-lesion," *Lasers Surg. Med.* **44**(9), 726–735 (2012).
10. R. A. Mesquita-Ferrari et al., "Effects of low-level laser therapy on expression of TNF-alpha and TGF-beta in skeletal muscle during the repair process," *Lasers Med. Sci.* **26**(3), 335–340 (2011).
11. X. Gao and D. Xing, "Molecular mechanisms of cell proliferation induced by low power laser irradiation," *J. Biomed. Sci.* **16**(1), 4 (2009).
12. W. P. Hu et al., "Helium-neon laser irradiation stimulates cell proliferation through photostimulatory effects in mitochondria," *J. Invest. Dermatol.* **127**(8), 2048–2057 (2007).
13. P. C. Silveira et al., "Evaluation of mitochondrial respiratory chain activity in muscle healing by low-level laser therapy," *J. Photochem. Photobiol. B* **95**(2), 89–92 (2009).
14. H. Toumi and T. Best, "The inflammatory response: friend or enemy for muscle injury?," *Br. J. Sports Med.* **37**, 284–286 (2003).
15. R. van den Berg et al., "Transcription factor NF-kappaB as a potential biomarker for oxidative stress," *Br. J. Nutr.* **86**(Suppl 1), S121–S127 (2001).
16. W. Lim et al., "The anti-inflammatory mechanism of 635 nm light-emitting-diode irradiation compared with existing COX inhibitors," *Lasers Surg. Med.* **39**(7), 614–621 (2007).
17. D. M. Iyomasa et al., "Ultrastructural analysis of the low level laser therapy effects on the lesioned anterior tibial muscle in the gerbil," *Micron* **40**(4), 413–418 (2009).
18. A. C. Amaral, N. A. Parizotto, and T. F. Salvini, "Dose-dependency of low-energy HeNe laser effect in regeneration of skeletal muscle in mice," *Lasers Med. Sci.* **16**(1), 44–51 (2001).
19. J. Nakano et al., "Low-level laser irradiation promotes the recovery of atrophied gastrocnemius skeletal muscle in rats," *Exp. Physiol.* **94**(9), 1005–1015 (2009).
20. T. A. Butterfield, T. M. Best, and M. A. Merrick, "The dual roles of neutrophils and macrophages in inflammation: a critical balance between tissue damage and repair," *J. Athl. Train.* **41**(4), 457–465 (2006).
21. Y. Li et al., "Transforming growth factor-beta1 induces the differentiation of myogenic cells into fibrotic cells in injured skeletal muscle: a key event in muscle fibrogenesis," *Am. J. Pathol.* **164**(3), 1007–1019 (2004).
22. M. D. Cressoni et al., "The effects of a 785-nm AlGaInP laser on the regeneration of rat anterior tibialis muscle after surgically-induced injury," *Photomed. Laser Surg.* **26**(5), 461–466 (2008).
23. L. Assis et al., "Low-level laser therapy (808 nm) contributes to muscle regeneration and prevents fibrosis in rat tibialis anterior muscle after cryolesion," *Lasers Med. Sci.* **28**(3), 947–955 (2013).
24. T. O. de Souza et al., "Phototherapy with low-level laser affects the remodeling of types I and III collagen in skeletal muscle repair," *Lasers Med. Sci.* **26**(6), 803–14 (2011).
25. J. A. Piva et al., "Effect of low-level laser therapy on the initial stages of tissue repair: basic principles," *An. Bras. Dermatol.* **86**(5), 947–954 (2011).
26. L. Ramos et al., "Infrared (810 nm) low-level laser therapy in experimental model of strain-induced skeletal muscle injury in rats: effects on functional outcomes," *Photochem. Photobiol.* **88**(1), 154–160 (2012).
27. J. T. Hashmi et al., "Effect of pulsing in low-level light therapy," *Lasers Surg. Med.* **42**(6), 450–466 (2010).
28. M. Mantineo, J. P. Pinheiro, and A. M. Morgado, "Evaluation of low level laser therapy irradiation parameters on rat muscle inflammation through systemic blood cytokines," *Proc. SPIE* **8932**, 89320M (2014).
29. W. O. P. Heine, *Environmental Management in Laboratory Animal Units: Basic Technology and Hygiene Methods and Practice*, PABST Science Publishers, Berlin (1998).
30. M. F. W. Festing et al., *The Design of Animal Experiments: Reducing the Use of Animals in Research Through Better Experimental Design*, Laboratory Animals Ltd., Ed., pp. 79–81, Royal Society of Medicine Press Ltd., London (2011).
31. European Commission, "Directive 2010/63/EU of the European Parliament and of the Council of 22 September 2010 on the protection of animals used for scientific purposes," <http://eur-lex.europa.eu/>

- [LexUriServ/LexUriServ.do?uri=OJ:L:2010:276:0033:0079:EN:PDF](#) (2010).
32. C. F. Rizzi et al., "Effects of low-level laser therapy (LLLT) on the nuclear factor (NF)-kappaB signaling pathway in traumatized muscle," *Lasers Surg. Med.* **38**(7), 704–713 (2006).
  33. K. R. Byrnes et al., "Light promotes regeneration and functional recovery and alters the immune response after spinal cord injury," *Lasers Surg. Med.* **36**(3), 171–185 (2005).
  34. T. I. Karu, "Multiple roles of cytochrome c oxidase in mammalian cells under action of red and IR-A radiation," *IUBMB Life*, **62**(8), 607–610 (2010).
  35. A. Gupta, T. Dai, and M. R. Hamblin, "Effect of red and near-infrared wavelengths on low-level laser (light) therapy-induced healing of partial-thickness dermal abrasion in mice," *Lasers Med. Sci.* **29**(1), 257–265 (2014).
  36. F. A. H. Al-Watban, X. Y. Zhang, and B. L. Andres "Low-level laser therapy enhances wound healing in diabetic rats: a comparison of different lasers," *Photomed. Laser Surg.* **25**(2), 72–77 (2007).
  37. M. Masoumpoor et al., "Effects of 660- and 980-nm low-level laser therapy on neuropathic pain relief following chronic constriction injury in rat sciatic nerve," *Lasers Med. Sci.* (2014) [Epub ahead of print].
  38. W. Qiuhe et al., "Low level laser therapy for traumatic brain injury," *Proc. SPIE* **7552**, 755206 (2010).
  39. Y.-Y. Huang et al., "Biphasic dose response in low level light therapy— an update," *Dose-Response* **9**(4), 602–618 (2011).
  40. K. P. Fernandes et al., "Effect of photobiomodulation on expression of IL-1beta in skeletal muscle following acute injury," *Lasers Med. Sci.* **28**(3), 1043–1046 (2013).
  41. S. Parasuraman, R. Raveendran, and R. Kesavan, "Blood sample collection in small laboratory animals," *J. Pharmacol. Pharmacother.* **1**(2), 87–93 (2010).
  42. M. F. Toft et al., "The impact of different blood sampling methods on laboratory rats under different types of anaesthesia," *Lab. Anim.* **40**(3), 261–274 (2006).
  43. PeptoTech Inc., "General Sandwich ELISA protocol," <https://www.peptotech.com/Lists/PTProtocol/Attachments/19/Sandwich%20ELISA%20-%20web.pdf> (2012).
  44. J. H. Zar, *Biostatistical Analysis*, Prentice-Hall International Inc., Englewood Cliff, New Jersey (1984).
  45. H. J. Gundersen et al., "Some new, simple and efficient stereological methods and their use in pathological research and diagnosis," *APMIS* **96**(1–6), 379–394 (1988).
  46. S. Jacques, T. Li, and S. Prael, "mcxyz.c, a 3D Monte Carlo simulation of heterogeneous tissues," <http://omlc.ogi.edu/software/mc/mcxyz/index.html> (2013).
  47. W. F. Cheong, S. A. Prael, and A. J. Welch, "A review of the optical-properties of biological tissues," *IEEE J. Quantum Electron.* **26**(12), 2166–2185 (1990).
  48. L. Oliveira et al., "The optical properties of rat abdominal wall muscle," Presented at *Workshop on Internet Biophotonics VI, Report 2, Saratov Fall Meeting 2013*, Saratov, Russia, <http://sfm.eventyry.org/report/713> (25–28 September 2013).
  49. R. Albertini et al., "Cytokine mRNA expression is decreased in the sub-plantar muscle of rat paw subjected to carrageenan-induced inflammation after low-level laser therapy," *Photomed. Laser Surg.* **26**(1), 19–24 (2008).
  50. N. A. Zhevago and K. A. Samoilova, "Pro- and anti-inflammatory cytokine content in human peripheral blood after its transcutaneous (*in vivo*) and direct (*in vitro*) irradiation with polychromatic visible and infrared light," *Photomed. Laser Surg.* **24**(2), 129–139 (2006).
  51. Y.-Y. Huang et al., "Biphasic dose response in low level light therapy," *Dose-Response* **7**(4), 358–383 (2009).
  52. P. Bolton, S. Young, and M. Dyson, "Macrophage responsiveness to light therapy: a dose response study," *Laser Ther.* **2**(3), 101–106 (1990).
  53. R. A. Lopes-Martins et al., "Spontaneous effects of low-level laser therapy (650 nm) in acute inflammatory mouse pleurisy induced by carrageenan," *Photomed. Laser Surg.* **23**(4), 377–381 (2005).
  54. P. R. Rich, A. J. Moody, and W. J. Ingledeu, "Detection of a near infrared absorption band of ferrohaem  $a_3$  in cytochrome c oxidase," *FEBS Lett.* **305**(3), 171–173 (1992).
  55. J. Joensen et al., "The thermal effects of therapeutic lasers with 810 and 904 nm wavelengths on human skin," *Photomed. Laser Surg.* **29**(3), 145–153 (2011).
  56. P. Brondon, I. Stadler, and R. J. Lanzafame, "Pulsing influences photo-radiation outcomes in cell culture," *Lasers Surg. Med.* **41**(3), 222–226 (2009).
  57. N. Lane, "Cell biology: power games," *Nature* **443**(7114), 901–903 (2006).
  58. R. Archid et al., "Confocal laser-scanning microscopy of capillaries in normal and psoriatic skin," *J. Biomed. Opt.* **17**(10), 101511. (2012).
  59. J. S. Nelson et al., "Laser pulse duration must match the estimated thermal relaxation time for successful photothermolysis of blood vessels," *Lasers Med. Sci.* **10**(1), 9–12 (1995).
  60. M. Brunori et al., "Internal electron transfer in Cu-heme oxidases: thermodynamic or kinetic control?" *J. Biol. Chem.* **272**(32), 19870–19874 (1997).

**Matias Mantineo** is a PhD student in biomedical engineering at the University of Coimbra, Portugal. He received his MD degree in bioengineering from the University of Mendoza, Argentina, in 2009. His current research interests include Laser–tissue interactions, clinical laser applications, photodynamic therapy, low-level laser therapy, and medical technology. He is a member of SPIE.

**João P. Pinheiro** is professor of medicine in the Faculty of Medicine of the University of Coimbra, specialist in physical and rehabilitation medicine and sports medicine and Head of the Physical and Rehabilitation Medicine Department in University Hospital of Coimbra. He is a member of the European Academy of Physical and Rehabilitation Medicine.

**António M. Morgado** received his PhD degree in physics and is assistant professor in the Department of Physics of the University of Coimbra. He is a researcher in IBILI—Institute for Biomedical Imaging and Life Sciences where in works mainly on the development of optoelectronic instrumentation and techniques for ocular imaging, namely corneal metabolic imaging using fluorescence lifetime microscopy, corneal confocal microscopy, and retinal OCT imaging. His research interests also include low-level laser therapy and laser safety. He is a member of SPIE.